BIOCHEMISTRY
including biophysical chemistry & molecular biology

Article

pubs.acs.org/biochemistry

Targeting the *de Novo* Biosynthesis of Thymidylate for the Development of a PET Probe for Pancreatic Cancer Imaging

Thushani D. Nilaweera,[†,‡] Muhammad Saeed,[†,§] and Amnon Kohen*

Department of Chemistry, University of Iowa, Iowa City, Iowa 52242, United States

ABSTRACT: The development of cancer-specific probes for imaging by positron emission tomography (PET) is gaining impetus in cancer research and clinical oncology. One of the hallmarks of most cancer cells is incessant DNA replication, which requires the continuous synthesis of nucleotides. Thymidylate synthase (TSase) is unique in this context because it is the only enzyme in humans that is responsible for the *de novo* biosynthesis of the DNA building block 2′-deoxythymidylate (dTMP). TSase catalyzes the reductive methylation of 2′-deoxy-uridylate (dUMP) to dTMP using (*R*)-N^5,N^{10}-methylene-5,6,7,8-tetrahydrofolate (MTHF) as a cofactor. Not surprisingly, several human cancers overexpress TSase, which makes it a common target for chemotherapy (e.g., 5-fluorouracil). We envisioned that [^{11}C]-MTHF might be a PET probe that could specifically label cancerous cells. Using stable radiotracer [^{14}C]-MTHF, we had initially found increased uptake by breast and colon cancer cell lines. In the current study, we examined the uptake of this radiotracer in human pancreatic cancer cell lines MIAPaCa-2 and PANC-1 and found predominant radiolabeling of cancerous versus normal pancreatic cells. Furthermore, uptake of the radiotracer is dependent on the intracellular level of the folate pool, cell cycle phase, expression of folate receptors on the cell membrane, and cotreatment with the common chemotherapeutic drug methotrexate (MTX, which blocks the biosynthesis of endogenous MTHF). These results point toward [^{11}C]-MTHF being used as PET probe with broad specificity and being able to control its signal through MTX co-administration.

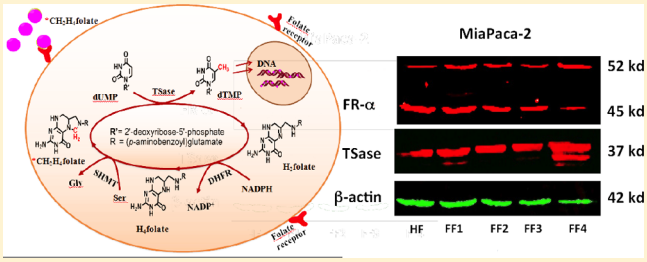

Positron emission tomography (PET) is a noninvasive molecular imaging tool used to acquire images based on the biological or metabolic function of the tissues of interest. Thus, in medicine, these images can provide crucial spatial and pathological information to oncologists to arrange effectual treatment plans and assess the progress of current treatment plans.[1−3] As a result, PET has potential applications in oncology and cancer research in which positron-emitting pharmaceutical probes are used in the imaging process. In general, a positron-emitting radioisotope, such as ^{11}C, ^{18}F, ^{13}N, ^{14}O, and ^{15}O, is substituted for a stable isotope of the pharmaceutical compound, and accumulation of the tracer in cancer cells, infection sites, or other tissues of interest is then monitored.[4−8]

Two common PET probes used in cancer imaging are [^{18}F]-fluorodeoxyglucose (FDG) and [^{18}F]-fluorothymidine (FLT). On the basis of the Warburg effect observed in cancer cells, the metabolic probe FDG is frequently used for cancer imaging. However, FDG is not a cancer-specific probe. Its absorption is high in numerous normal tissues with high metabolic rates in organs such as the brain, heart, kidney, and areas of inflammation.[9] In contrast, FLT is a proliferation marker, which exploits the salvage pathway for the maintenance of intracellular thymidylate in certain cancers.[10] Unfortunately, the detected levels of FLT are not always reliable, and the accuracy of both FDG and FLT is limited.[11,12] Another common drawback of fluorinated radiopharmaceuticals is their potential to defluorinate *in vivo*[13] and their activity in inhibiting several biological pathways.

Compared to the salvage pathway targeted by FLT, *de novo* synthesis of thymidine (Figure 1) is ubiquitous in fast proliferating cells. FLT relays the expression of thymidine kinase (TdK), whereas the targeted *de novo* biosynthesis of thymidine relays the enhanced expression of folate receptors (FRs) and the enzyme thymidylate synthase (TSase; EC 2.1.1.45). Consequently, developing a PET probe targeting *de novo* synthesis will target different types of cancers and will complement FLT as a diagnostic tool. Recently, we reported the synthesis of ^{11}C-labeled (*R*)-N^5,N^{10}-methylene-5,6,7,8-tetrahydrofolate ([^{11}C]-MTHF),[14] the cofactor of TSase. Furthermore, in tissue culture studies, we reported that cancer cells are predominantly labeled compared to their normal counterparts using [^{14}C]-MTHF, a stable isotopologue of [^{11}C]-MTHF.[15]

FRs and TSase play vital roles in the uptake and retention of radiolabeled MTHF; FRs transport folates, including MTHF, into the cell where the enzyme TSase then transfers the radiolabeled methylene moiety to the precursor 2′-deoxyuridine-5′-monophosphate (dUMP). The catalytic conversion of dUMP to 2′-deoxythymidine-5′-monophosphate (dTMP) is a crucial step in the *de novo* biosynthesis of the base thymidine in

Received: December 3, 2014
Revised: January 6, 2015
Published: January 12, 2015

DOI: 10.1021/bi501481n
Biochemistry 2015, 54, 1287−1293

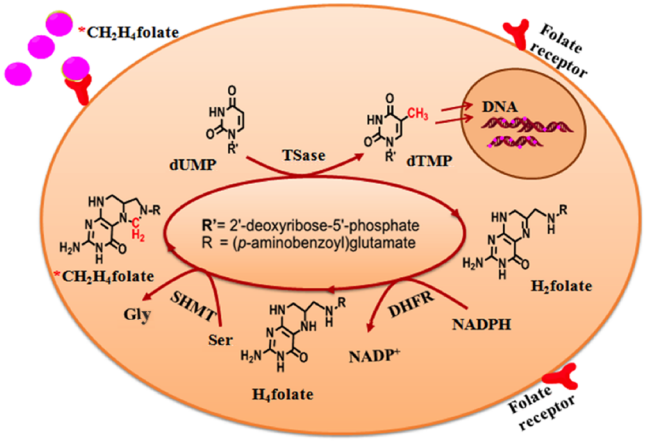

Figure 1. Schematic representation of targeting the *de novo* synthesis of thymidine in folate overexpressed and DHFR inhibited cells by an ^{11}C radiotracer. [^{11}C]-MTHF is transported into cells via folate receptors (Fr-α), and [^{11}C]-radionuclide is transferred into dUMP by TSase and converted into [^{11}C]-dTMP.

humans.[16−18] Importantly, several cancers are known to overexpress FRs, including folate receptor-α (FR-α) and TSase.[19−21] Specifically, human pancreatic cancer cells overexpress FRs and TSase,[22−24] suggesting that they can serve as double selection targets for pancreatic cancer imaging. However, the cellular pool of folate is maintained in equilibrium with several other folate derivatives by folate recycling enzymes (e.g., dihydrofolate reductase, DHFR). Therefore, the cells' dependency on the extracellular supply of MTHF depends on DHFR activity and endogenous MTHF production. In this article, we tested the uptake of MTHF by cancerous pancreatic cell lines relative to normal cell lines as a function of global intracellular folate pools and an inhibited folate regenerating system.

EXPERIMENTAL PROCEDURES

Materials. [^{14}C]-Formaldehyde ($^{14}CH_2O$, 50 mCi/mmol, 1−3% aqueous solution) was purchased from Moravek Biochemicals. (6*S*)-5,6,7,8-Tetrahydrofolate (THF) and N^5,N^{10}-methylene-5,6,7,8-tetrahydrofolate (MTHF) were a generous gift from Eprova-Merck. Preparation of [^{14}C]-MTHF was accomplished by mixing a solution of $^{14}CH_2O$ (50 μL) and THF (2 mg) in 100 μL of folate-stabilizing buffer. Folate-stabilizing buffer was prepared by dissolving 40 mg of ascorbic acid and 60 mg of trisodium citrate dihydrate in 10 mL of argon-purged water.

Cell Culture. Pancreatic cancer cell lines (MIAPaCa-2 and PANC-1) and primary pancreatic cells (H6c7) were kindly provided by Douglas Spitz and Joseph Cullen (University of Iowa), respectively. All cell cultures were conducted in 10 cm^2 culture plates in an incubator maintained at 37 °C under an atmosphere of 5% CO_2 and 95% air. Cells in log phase growth were passed or selected for uptake experiments when they were ∼70% confluent as described previously.[15] Primary pancreatic cells were grown in KSFM medium (Invitrogen) supplemented with EGF (2.5 μg), bovine pituitary extract (25 mg), 50 IU/mL penicillin, and 50 μg/mL streptomycin. The cancer cells were initially grown in regular high-folate (2.3 μM) RPMI 1640 medium (HF, Invitrogen) supplemented with 10% heat-inactivated FBS, 1% glutamine, 50 IU/mL penicillin, and 50 μg/mL streptomycin. The cancer cells were then adapted in folate-free RPMI 1640 medium (FF, Invitrogen) supplemented with 10% heat-inactivated dialyzed FBS (Invitrogen), 1% glutamine, 50 IU/mL penicillin, and 50 μg/mL streptomycin. Adaptation was started by placing the cells, originally grown in HF medium, in a medium containing a 1:1 HF/FF mixture (FF1 population) for 3 days. The FF1 population was then split 1:3 and passed in 100% FF medium for 3 days (FF2). Next, passages were maintained in FF medium until a growth arrest stage was achieved (∼FF6). For labeling studies, cell cycle analyses, and western blot analyses, cells were used when culture plates were ∼65−75% confluent.

[^{14}C]-MTHF Uptake by Cells. The uptake medium (30 mL) was prepared by supplementing FF medium with MTHF (20 μM final concentration) containing ∼0.5 μCi of [^{14}C]-MTHF. For MIAPaCa-2 cancer cells, which presented with loosely attached live cells in culture, suspended cells were retrieved by collecting and centrifuging the medium in 15 mL tubes. After the supernatant was removed, the cell pellet was suspended in labeling medium (3 mL/plate) and returned to the respective plate with attached cells. For PANC-1 cells, which have no suspended cells, the growth medium was aspirated and replaced by labeling medium (3 mL). For normal pancreatic H6c7 cells, the growth medium was aspirated; the cells were briefly (30 min) incubated with FF medium to remove any folate bound to the plasma membrane, and uptake medium was added. Cultures were incubated at 37 °C for 90 min in uptake medium. Then, the culture plates were immediately placed on ice; the labeling medium was aspirated, and the cells were washed twice with ice-cold 1× PBS. The cells were detached with 0.25% trypsin-EDTA at room temperature, suspended in 0.5 mL of PBS, and counted using a Bio-Rad TC20 automated cell counter. The cells were then transferred to scintillation vials, lysed in 0.5 mL of 0.5% SDS, mixed with 10 mL of scintillation fluid, and counted in a liquid scintillation counter (LSC) for 5 min using the ^{14}C window (0−156 keV). All of the uptake experiments were conducted in two independent experiments in triplicate for each (6 total samples), and the flow cytometer measurements consisted of two independent experiments in duplicate for each (4 total samples). The error bars in all of the figures represent the standard deviation of those measurements from the average.

Effect of Methotrexate (MTX) Treatment on Uptake of the Radiotracer. Cancer cells maintained at various passages, including HF and FF1−FF4, were tested for MTX-based enhancement of radioactivity uptake and retention. Growth media from the cultures were aspirated and replaced with FF media supplemented with MTX at different concentrations and incubated for different amounts of time. For time-dependent experiments, the cells were treated with 10 nM MTX for 15, 30, 45, 60, 120, and 180 min. For dose-dependent experiments, MTX concentrations of 1, 3, 5, 10, 50, and 100 nM were used, and the cultures were incubated for 30 min. After incubation, MTX-containing media were removed, and the cells were washed twice with 1× PBS. Then, the cells were immediately placed in the uptake media as described above. For control experiments, the cells were incubated with solvent (no MTX) followed by incubation in the labeling medium as described above.

Cell Cycle Analysis. Cancer cells maintained at various passages, including HF and FF1−FF4, were used for cell cycle analyses. The cells were harvested with trypsin, washed twice with cold 1× PBS, and suspended at a density of 1 × 10^6 cells/mL in PBS. The cells were fixed overnight with ethanol at a

DOI: 10.1021/bi501481n
Biochemistry 2015, 54, 1287−1293

concentration of 70% at −20 °C. The cells were harvested from the alcohol suspension by centrifugation and resuspended in propidium iodide (PI) stain (1 mL). PI staining buffer consisted of PI (5 μg/mL), RNase A (1 mg/mL), and glucose (1 mg/mL) in PBS. The stained cells were filtered through a 70 μm nylon strainer and analyzed for DNA content on a FACScan flow cytometer (BD Biosciences) using FlowJo software. The data were analyzed using FlowJo 8.8.7 software.

Western Blot Analysis of Folate Receptor-α (FR-α) and TSase Enzyme. The culture medium of the cells in log phase was collected in 15 mL tubes and centrifuged to collect the suspended cells. The detached cells were washed twice with cold PBS and harvested on ice with 200 μL of lysis buffer containing 1% Triton X-100, 150 mM NaCl, 0.5% sodium deoxycholate, and 0.1% SDS in 50 mM Tris at pH 8.0. To inhibit proteasome degradation of proteins, a tablet of complete mini EDTA-free protease inhibitor cocktail (Roche) was added to the lysis buffer. The extract was incubated on ice for 20 min, passed through a 25 gauge needle, and finally centrifuged at 15000*g* for 20 min at 4 °C. The supernatant was removed in a 1.5 mL tube, and the protein concentration was measured using a BCA protein kit. A protein sample of 50 μg was loaded and electrophoresed on 10% SDS-polyacrylamide gels. Size standards from 10 to 250 kDa (Bio-Rad Kaleidoscope) were included. Polypeptides were electro-transferred to nitrocellulose membranes. The membranes were blocked with Odyssey blocking buffer (Li-Cor) and probed with anti-human folate receptor or anti-human TSase antibody (Santa Cruz Biotechnology). For visualization, anti-species secondary antibodies labeled with AlexaFluor 680 or AlexFluor 800 were used. The membranes were blotted on a Li-Cor Odyssey scanner.

RESULTS AND DISCUSSION

Uptake of [^{14}C]-MTHF by Primary and Cancerous Pancreatic Cells. The radiotracer [^{14}C]-MTHF was used to distinguish between cancerous and normal pancreatic cells and to test whether uptake of radioactivity can be enhanced by treatment with MTX. We selected two pancreatic cancer cell lines (MIAPaCa-2 and PANC-1) and compared their uptake of radiotracer to that of normal pancreatic H6c7 cells. Both the normal and cancerous cells were grown in their recommended media and selected for uptake experiments during log phase growth (65−75% confluent). Prior to the experiment, the cells were briefly incubated with FF medium to wash away folates from the media that were attached to the plasma membrane and then incubated in the labeling medium supplemented with 20 μM MTHF containing 0.05 μCi of [^{14}C]-MTHF tracer for 90 min at 37 °C. The amount of radiotracer taken up by the cells was determined by LSC and normalized to the total cell number and initial dose of radioactivity using the following formula.

$$\text{normalized uptake} = \frac{\text{cpm recorded in cells}}{\text{cpm added} \times \text{total cells} \times 10^{-6}}$$

As shown in Figure 2, accumulation of radiotracer in primary pancreatic H6c7 cells was less than that in either cancer cell line. The uptake of radiotracer by MIAPaCa-2 cells was ∼3-fold higher than that of normal pancreatic cells. On the other hand, accumulation of tracer in PANC-1 cells was ∼7-fold higher than that of normal cells and almost double the level observed in the MIAPaCa-2 cell line. These results indicate that [^{14}C]-MTHF not only can distinguish between normal and cancerous cells but also may be used to distinguish between these pancreatic cancer cell lines.

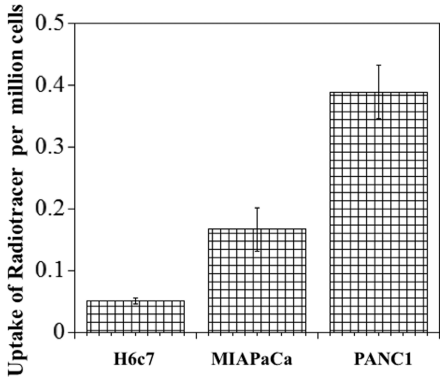

Figure 2. [^{14}C]-MTHF uptake in normal and cancerous cells of pancreatic origin.

Uptake of [^{14}C]-MTHF by Cancerous Cells Grown in FF Medium. The regular HF medium for growing MIAPaCa-2 and PANC-1 cells contains ∼2.3 μM folates, which is ∼100-fold higher than the physiological concentration found in humans.[25] Although culture media with such a high nonphysiological concentration of folates offer significant growth advantages, it also leaves the cells with abnormally high intracellular pools of folates. In such artificially high folate media, the expression of folate transporting proteins on the plasma membrane and overall, including FR, would be reduced. By lowering the concentration of intracellular folates close to physiological levels (nM), we hope to better assess the potential of the radiotracer *in vivo*. To test this hypothesis, we adapted both pancreatic cancer cell lines (MIAPaCa-2 and PANC-1) to FF medium for up to six passages (FF6). We observed continuous growth retardation starting at passage FF2 with complete arrest at passage FF6. Adaptation of normal pancreatic H6c7 cells was not successful as the cells' growth was arrested in FF medium at the FF1 stage.

Figure 3 shows uptake of the [^{14}C]-MTHF tracer in MIAPaCa-2 and PANC-1 cells grown in HF and FF media.

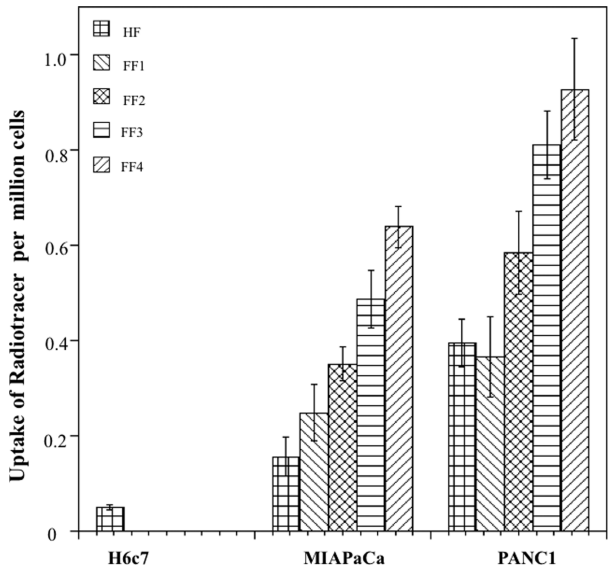

Figure 3. Uptake of [^{14}C]-MTHF by pancreatic cancer cells grown in HF or FF medium relative to normal pancreatic cells.

DOI: 10.1021/bi501481n
Biochemistry 2015, 54, 1287−1293

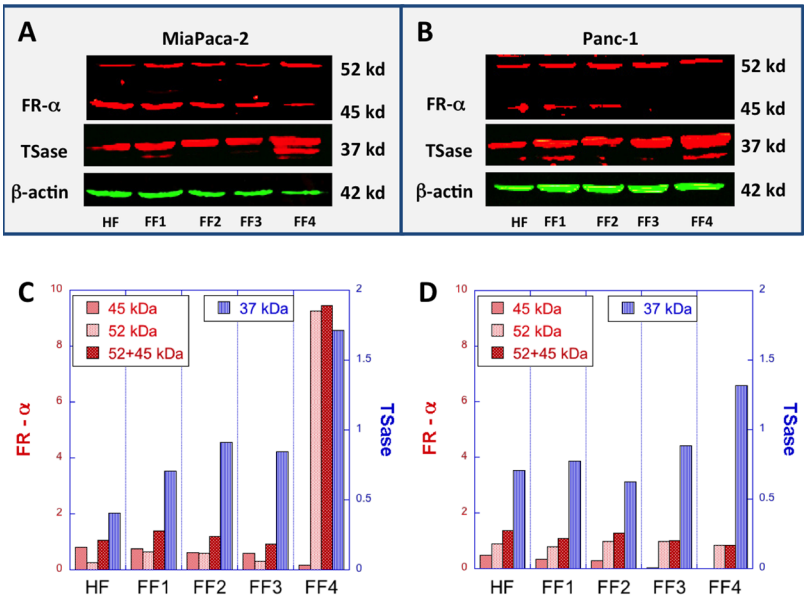

Figure 4. Western blot analysis of FR-α and TSase expression in (A) MIAPaCa-2 and (B) PANC-1 cancer cells. (C) Analysis of MIAPaCa-2 cells with FR-α (red) and TSase (blue) normalized relative to β-actin. (D) Analysis of PANC-1 cells with FR-α (red) and TSase (blue) normalized relative to β-actin.

As expected, cells grown in FF medium had enhanced uptake of the radiotracer. Enhancement was more prominent in MIAPaCa-2 cells, where uptake of the radiotracer at passage FF4 was almost 4-fold higher than that of the cells grown in HF medium. In the case of PANC-1 cells, the enhancement of radiotracer uptake at passage FF4 was only 2-fold higher compared to that of the cells grown in HF medium. When compared to the uptake by primary pancreatic cells, the MIAPaCa-2 and PANC-1 cells at passage FF4 have almost 12- and 18-fold enhancement, respectively (Figure 3). This enhancement clearly indicates that the cells grown in low folate medium have more dependence on exogenous sources of folate.

Effect of the Level of FR-α and TSase Protein Expression on the Uptake of [^{14}C]-MTHF. Western blots were used to test the dependence of [^{14}C]-MTHF uptake on the expression of FR-α and TSase proteins in MIAPaCa-2 and PANC-1 cell lines grown under high- and low-folate conditions. The radioactive methylene in labeled MTHF is trapped in cells by reductive methylation of dUMP to form dTMP, which is catalyzed by TSase. Expression of this enzyme is also enhanced in FF medium (Figure 4), which further enhances uptake of [^{14}C]-MTHF radioactivity in the cells. Shown in Figure 4 for MIAPaCa-2 cells, two bands were observed when the membranes were exposed to anti-FR-α antibody (FL-257, Santa Cruz). The band at ~45 kDa, which corresponds to FR-α, remained expressed in both HF and FF media. Adaptation of MIAPaCa-2 cells to FF medium decreased the expression of this band sequentially, and ~78% of the protein expressed in HF medium was lost in the FF4 passage population. Interestingly, we observed another band at 52 kDa that had increasing expression in the FF passages. We observed that expression of this protein at passage FF4 was enhanced ~9-fold compared to the expression level in HF medium. This peak is likely to be the mature FR receptor with a post-transcriptional modification. Taken together, there is enhanced expression of FRs in cells adapted to FF medium (Figure 4C and D, 52 and 45 kDa bands combined), and this trend correlates positively with the uptake of radiolabeled external folate by MIAPaCa-2 cells.

Similar trends with slight variations in the expression profiles were observed in PANC-1 cells, where the cells showed an FR-α band at 45 kDa until passage FF2, which was then completely absent in passages FF3 and FF4. In contrast to that observed for MIAPaCa-2 cells, the 52 kDa band was constitutively expressed in all passages for PANC-1 cells and became the only band seen after passage FF3. The analysis showed induced expression of TSase when both cell lines were adapted to FF medium. Up to 4-fold enhancement in the expression of TSase was observed in the FF4 population of MIAPaCa-2 cells, whereas this enhancement was modest (~2-fold) in PANC-1 cells (Figure 4C and D). These data indicated that the enhancement of [^{14}C]-MTHF uptake at passage FF4 (Figure 3) depends on the expression of either folate receptors on cell membranes or TSase expression in the cytoplasm.

Effect of Intracellular Recycling of Folate on the Uptake of [^{14}C]-MTHF. The intracellular folate pool is maintained by the folate cycle (Figure 1), which involves catalytic conversion of folic acid and dihydrofolate (DHF) to tetrahydrofolate (THF) by dihydrofolate reductase (DHFR). Cytosolic serine hydroxymethyltransferase (cSHMT) then catalyzes the transfer of a hydroxymethyl group from serine to furnish a methylene ($-CH_2-$) moiety for the formation of MTHF from THF. Thus, inhibition of DHFR is likely to reduce endogenous production of MTHF and to increase the cells' dependence on exogenous, radiolabeled MTHF. To test this hypothesis, we used MTX, a pyrimethamine inhibitor of DHFR and common chemotherapeutic drug.[26] MIAPaCa-2 and PANC-1 cells were treated with MTX (10 nM) for 30 min prior to incubation with [^{14}C]-MTHF uptake medium. Because uptake of the radiotracer by the cells in passages FF1 and FF2 was relatively similar to the uptake in HF medium, we compared the effects of MTX treatment in HF and FF media in passages FF3 and FF4. Cells at the same FF passages but without MTX pretreatment were used as controls.

DOI: 10.1021/bi501481n
Biochemistry 2015, 54, 1287−1293

The results are shown in Figure 5. Labeling of the cells grown in HF medium does not show significant enhancement

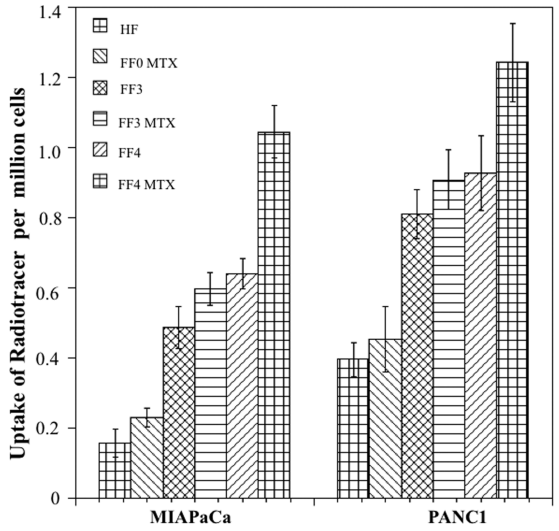

Figure 5. Effect of MTX on the uptake of [^{14}C]-MTHF by pancreatic cancer cells.

due to MTX treatment. This observation seems obvious when one considers the high concentration of folic acid in the HF medium (2.3 μM), which competes for uptake of MTX by the same folate transporting proteins. The cells adapted to FF medium at passage FF3 also did not show significant enhancement in the uptake of radiotracer. This observation might be attributable to a sufficient concentration of intracellular THF and insufficient expression of folate transporting proteins, including FR-α, at passage FF3. The cells in passage FF4, on the other hand, showed ~30% enhancement of radiotracer uptake in MIAPaCa-2 and PANC-1 cells in response to the MTX treatment. The uptake enhancement of the radiotracer pointed toward the role of intracellular and extracellular pools of folates, which can be used as a marker to label cells with a strong demand for folates. This outcome also supports the proposed mechanism of radioactivity trapping in the cell as presented above.

Cell Cycle Analysis. One hallmark of cancer is aggressive proliferation, which involves the synthesis of new daughter DNA strands in the S phase of the cell cycle. Under such conditions, extensive synthesis of nucleotides including dTMP is required. Consequently, we studied the correlation between MTHF uptake and the cell cycle. The cells were first fixed in alcohol, as described in Experimental Procedures, and then analyzed using a FACScan flow cytometer.

As is apparent in Figure 6, the population in the G1 phase increased with a concomitant decrease of cells in the S phase. However, a small fraction of cells (~20%) was always present in the G2/M phase, indicating a slow but steady growth rate. For breast and colon cells, we have reported that cells passing through the S phase incorporate more MTHF.[14] However, in this study of pancreatic cancer cells, the S phase of cells was gradually decreased, whereas the G0/G1 phase increased from FF0 to FF4. However, the [^{14}C]-MTHF uptake was higher in FF-adopted cells in which passage FF4 had the highest uptake in both cell lines. Thus, MTHF uptake does not directly correlate with the S phase of the cell cycle in MIAPaCa-2 and PANC-1 cell lines. This phenomenon probably results from a trade-off between cells adapting to low folate by moving into the G0 phase on one hand and increased dependence on exogenous MTHF at the S phase on the other hand.

CONCLUSION

These findings demonstrate that [^{14}C]-MTHF radiolabeling of pancreatic cancer cells is significantly higher than that for normal pancreatic cells. Uptake of the radiotracer increases with the dependence of the cells on exogenous MTHF, which is associated with higher expression of folate receptors on the cell membrane, the expression of TSase, the cell cycle phase, and MTX inhibition of the endogenous production of MTHF. Apparently, the depletion of folates in media to their presumed *in vivo* level led to depleted intracellular levels of folates, and the cells appear to depend more on extracellular folate resources and thus overexpress FR and TSase to overcome folate

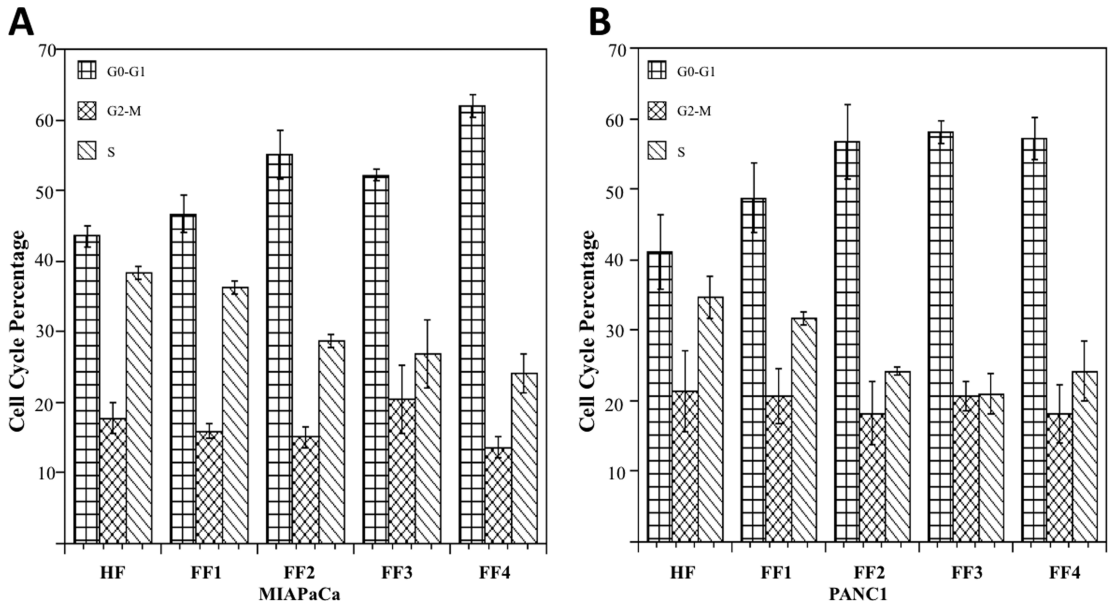

Figure 6. Cell cycle analysis of (A) MIAPaCa-2 cells and (B) PANC-1 cells grown in HF or FF medium.

DOI: 10.1021/bi501481n
Biochemistry 2015, 54, 1287−1293

starvation. In addition to endogenous folate depletion, inhibition of the intracellular folate recycling path by the common chemotherapeutic agent MTX, a DHFR inhibitor, also directed cells to rely more on extracellular folates and enhanced radiolabeling with [^{14}C]-MTHF. Overall, these findings point toward the proposed PET probe [^{11}C]-MTHF having specificity for cancerous pancreatic tissues and could potentially be exploited to image pancreatic cancer cells with low intracellular folate levels and overexpressed FR and TSase. Additionally, because MTX is FDA approved, and could be administered to cancer patients in small doses prior to a PET procedure, it is possible that it could enhance radiotracer uptake by pancreatic cancers and thus improve the signal to noise ratio of the PET image.

AUTHOR INFORMATION

Corresponding Author

*E-mail: Amnon-kohen@uiowa.edu. Phone: 319-315-0234. Fax: 319-315-1270.

Present Addresses

‡T.D.N.: Department of Chemistry, University of Virginia, McCormick Road, P.O. Box 400319, Charlottesville, VA 22904-4319, United States.

§M.S.: Department of Chemistry, SBA School of Science and Engineering, Lahore University of Management Sciences (LUMS), D.H.A. Phase II, Lahore 54792, Pakistan.

Author Contributions

†T.D.N. and M.S. contributed equally to this work.

Funding

This research was funded in part by NIH Grant RO1 GM65368, a pilot grant from the Institute of Clinical and Translational Science, and a grant from the Biological Science Funding Program from the University of Iowa.

Notes

The authors declare no competing financial interest.

ABBREVIATIONS

DHFR, dihydrofolate reductase; dTMP, 2′-deoxythymidine-5′-monophosphate; dUMP, 2′-deoxyuridine-5′-monophosphate; FDG, 2′-deoxy-2′-[^{18}F]-fluoroglucose; FF, folate-free medium; FLT, 3′-deoxy-3′-[^{18}F]-fluorothymidine; FRs, folate receptors; MTHF, (*R*)-N^5,N^{10}-methylene-5,6,7,8-tetrahydrofolate; MTX, methotrexate; PET, positron emission tomography; TdK, thymine kinase; TSase, thymidylate synthase

REFERENCES

(1) van der Meel, R., Gallagher, W. M., Oliveira, S., O'Connor, A. E., Schiffelers, R. M., and Byrne, A. T. (2010) Recent advances in molecular imaging biomarkers in cancer: application of bench to bedside technologies. *Drug Discovery Today 15*, 102−114.

(2) Juweid, M. E., and Cheson, B. D. (2006) Positron-emission tomography and assessment of cancer therapy. *N. Engl. J. Med. 354*, 496−507.

(3) Bouchelouche, K., Capala, J., and Oehr, P. (2009) Positron emission tomography/computed tomography and radioimmunotherapy of prostate cancer. *Curr. Opin. Oncol. 21*, 469−474.

(4) Ullrich, R. T., Kracht, L., Brunn, A., Herholz, K., Frommolt, P., Miletic, H., Deckert, M., Heiss, W. D., and Jacobs, A. H. (2009) Methyl-L-^{11}C-methionine PET as a diagnostic marker for malignant progression in patients with glioma. *J. Nucl. Med. 50*, 1962−1968.

(5) Song, W. S., Nielson, B. R., Banks, K. P., and Bradley, Y. C. (2009) Normal organ standard uptake values in carbon-11 acetate PET imaging. *Nucl. Med. Commun. 30*, 462−465.

(6) Timmers, H. J., Chen, C. C., Carrasquillo, J. A., Whatley, M., Ling, A., Havekes, B., Eisenhofer, G., Martiniova, L., Adams, K. T., and Pacak, K. (2009) Comparison of ^{18}F-fluoro-L-DOPA, ^{18}F-dluoro-deoxyglucose, and ^{18}F-fluorodopamine PET and ^{123}I-MIBG scintigraphy in the localization of pheochromocytoma and paraganglioma. *J. Clin. Endocrinol. Metab. 94*, 4757−4767.

(7) Xiangsong, Z., Xinjian, W., Yong, Z., and Weian, C. (2008) ^{13}N-NH_3: a selective contrast-enhancing tracer for brain tumor. *Nucl. Med. Commun. 29*, 1052−1058.

(8) Lodge, M. A., Jacene, H. A., Pili, R., and Wahl, R. L. (2008) Reproducibility of tumor blood flow quantification with ^{15}O-water PET. *J. Nucl. Med. 49*, 1620−1627.

(9) Nair, V. S., Krupitskaya, Y., and Gould, M. K. (2009) Positron emission tomography ^{18}F-fluorodeoxyglucose uptake and prognosis in patients with surgically treated, stage I non-small cell lung cancer: a systematic review. *J. Thorac. Oncol. 4*, 1473−1479.

(10) Bradbury, M. S., Hambardzumyan, D., Zanzonico, P. B., Schwartz, J., Cai, S., Burnazi, E. M., Longo, V., Larson, S. M., and Holland, E. C. (2008) Dynamic small-animal PET imaging of tumor proliferation with 3′-deoxy-3′-^{18}F-fluorothymidine in a genetically engineered mouse model of high-grade gliomas. *J. Nucl. Med. 49*, 422−429.

(11) Troost, E. G., Vogel, W. V., Merkx, M. A., Slootweg, P. J., Marres, H. A., Peeters, W. J., Bussink, J., van der Kogel, A. J., Oyen, W. J., and Kaanders, J. H. (2007) ^{18}F-FLT PET does not discriminate between reactive and metastatic lymph nodes in primary head and neck cancer patients. *J. Nucl. Med. 48*, 726−735.

(12) Honer, M., Ebenhan, T., Allegrini, P. R., Ametamey, S. M., Becquet, M., Cannet, C., Lane, H. A., O'Reilly, T. M., Schubiger, P. A., Sticker-Jantscheff, M., Stumm, M., and McSheehy, P. M. (2010) Anti-angiogenic/vascular effects of the mTOR inhibitor everolimus are not detectable by FDG/FLT-PET. *Translational Oncology 3*, 264−275.

(13) Shetty, H. U., Zoghbi, S. S., Simeon, F. G., Liow, J.-S., Brown, A. K., Kannan, P., Innis, R. B., and Pike, V. W. (2008) Radiodefluorination of 3-fluoro-5-(2-(2-[^{18}F](fluoromethyl)-thiazol-4-yl)-ethynyl)benzonitrile ([^{18}F]SP203), a radioligand for imaging brain metabotropic glutamate subtype-5 receptors with positron emission tomography, occurs by glutathionylation in rat brain. *J. Pharmacol. Exp. Ther. 327*, 727−735.

(14) Saeed, M., Tewson, T. J., Erdahl, C. E., and Kohen, A. (2012) A fast chemoenzymatic synthesis of [^{11}C]-N^5,N^{10}-methylenetetrahydrofolate as a potential PET tracer for proliferating cells. *Nucl. Med. Biol. 39*, 697−701.

(15) Saeed, M., Sheff, D., and Kohen, A. (2011) Novel positron emission tomography tracer distinguishes normal from cancerous cells. *J. Biol. Chem. 286*, 33872−33878.

(16) Carreras, C. W., and Santi, D. V. (1995) The catalytic mechanism and structure of thymidylate synthase. *Annu. Rev. Biochem. 64*, 721−762.

(17) Agrawal, N., Hong, B., Mihai, C., and Kohen, A. (2004) Vibrationally enhanced hydrogen tunneling in the *Escherichia coli* thymidylate synthase catalyzed reaction. *Biochemistry 43*, 1998−2006.

(18) Hong, B., Maley, F., and Kohen, A. (2007) Role of Y94 in proton and hydride transfers catalyzed by thymidylate synthase. *Biochemistry 46*, 14188−14197.

(19) Cagle, P. T., Zhai, Q. J., Murphy, L., and Low, P. S. (2013) Folate receptor in adenocarcinoma and squamous cell carcinoma of the lung: potential target for folate-linked therapeutic agents. *Arch. Pathol. Lab. Med. 137*, 241−244.

(20) Lindebjerg, J., Nielsen, J. N., Hoeffding, L. D., Bisgaard, C., Brandslund, I., and Jakobsen, A. (2006) Expression of thymidylate synthase in primary colorectal adenocarcinoma. *Appl. Immunohistochem. Mol. Morphol. 14*, 37−41.

(21) Yu, Z., Sun, J., Zhen, J., Zhang, Q., and Yang, Q. (2005) Thymidylate synthase predicts for clinical outcome in invasive breast cancer. *Histol. Histopathol. 20*, 871−878.

(22) van der Zee, J. A., van Eijck, C. H., Hop, W. C., van Dekken, H., Dicheva, B. M., Seynhaeve, A. L., Koning, G. A., Eggermont, A. M., and Ten Hagen, T. L. (2012) Expression and prognostic significance of

DOI: 10.1021/bi501481n
Biochemistry 2015, 54, 1287−1293

thymidylate synthase (TS) in pancreatic head and periampullary cancer. *European Journal of Surgical Oncology 38*, 1058−1064.
(23) Ruiz-Tovar, J., Fernandez-Contreras, M. E., Martin-Perez, E., and Gamallo, C. (2012) Association of thymidylate synthase and hypoxia inducible factor-1alpha DNA polymorphisms with pancreatic cancer. *Tumori 98*, 364−369.
(24) Liong, M., Lu, J., Kovochich, M., Xia, T., Ruehm, S. G., Nel, A. E., Tamanoi, F., and Zink, J. I. (2008) Multifunctional inorganic nanoparticles for imaging, targeting, and drug delivery. *ACS Nano 2*, 889−896.
(25) Kane, M. A., Roth, E., Raptis, G., Schreiber, C., and Waxman, S. (1987) Effect of intracellular folate concentration on the modulation of 5-fluorouracil cytotoxicity by the elevation of phosphoribosylpyrophosphate in cultured human KB cells. *Cancer Res. 47*, 6444−6450.
(26) Olsen, E. A. (1991) The pharmacology of methotrexate. *J. Am. Acad. Dermatol. 25*, 306−318.

DOI: 10.1021/bi501481n
Biochemistry 2015, 54, 1287−1293